Tunneling conductance of connected carbon nanotubes

R. Saito
Department of Electronics Engineering, University of Electro-Communications, Chofugaoka, Chofu, 182 Tokyo, Japan

G. Dresselhaus
Francis Bitter National Magnet Laboratory, Massachusetts Institute of Technology, Cambridge, Massachusetts 02139

M. S. Dresselhaus
Department of Electrical Engineering and Computer Science and Department of Physics, Massachusetts Institute of Technology, Cambridge, Massachusetts 02139

(Received 4 August 1995; revised manuscript received 2 October 1995)

A three-dimensional structure of two carbon nanotubes (CN) joined by a connecting region containing a pentagon and heptagon pair is given by the use of a projection method. The connecting joint is uniquely determined for the given two chiral vectors of CN by a vector which defines a three-dimensional dihedral angle. The tunneling conductance is calculated for a metal-metal CN junction and a metal-semiconducting CN junction. The calculated results clearly show that these junctions work as the smallest semiconductor devices.

I. INTRODUCTION

Carbon nanotubes (CN's) have been investigated intensively as a different form of a one-dimensional material.[1] Carbon nanotubes consist of a rolled-up graphene sheet, the geometry, e.g., the diameter and chirality, of which can be changed without introducing any impurity or deformation, except for the curvature of the tube.[2] Thus, the physical properties of carbon nanotubes can be understood as those of a two-dimensional graphene sheet, with periodic boundary conditions in the circumferential direction of the tube. The electronic structure of a carbon nanotube can be either metallic or semiconducting, depending on diameter and chirality[3–7] which can be uniquely determined by the chiral vector, C_h,

$$C_h = n\vec{a}_1 + m\vec{a}_2 \equiv (n,m), \tag{1}$$

where $\vec{a}_1$ and $\vec{a}_2$ are unit vectors of a two-dimensional graphene sheet (see Fig. 1) and n, m are integers. If we neglect the small gap [on the order of 10 meV for the smallest diameter metallic CN (Refs. 4 and 6)], due to the effect of the tube curvature, metallic or semiconducting tubes are obtained depending on whether or not n-m is a multiple of 3, respectively.[5] The energy gap for a semiconducting tube is inversely proportional to the tube diameter (independent of the chirality) and is on the order of 1 eV for the smallest diameter (~ 7 Å) nanotube.[8]

An interesting system for studying the coexistence of metallic and semiconducting nanotubes concerns the design of a metal-semiconducting device by connecting metal and semiconducting tubes to each other with a junction region containing only carbon pentagons, hexagons, and heptagons. Hereafter, for simplicity, we denote a pentagonal or heptagonal carbon ring as a pentagon or a heptagon, respectively. Though it seems difficult to connect two honeycomb networks of different diameters and chiralities, a pentagon and heptagon pair makes it possible to connect two nanotubes of different diameters and chiralities. Such connections have been directly observed by Iijima and others in transmission electron microscope (TEM) experiments.[9] Comparing the measured angle in the TEM experiments at the kink in the tube joint with a model of carbon nanotubes in which a pentagon and heptagon pair changes the tube diameter (see, for example, Fig. 2), the junction shape can be fit to the TEM experiments. Endo and many other groups have reported

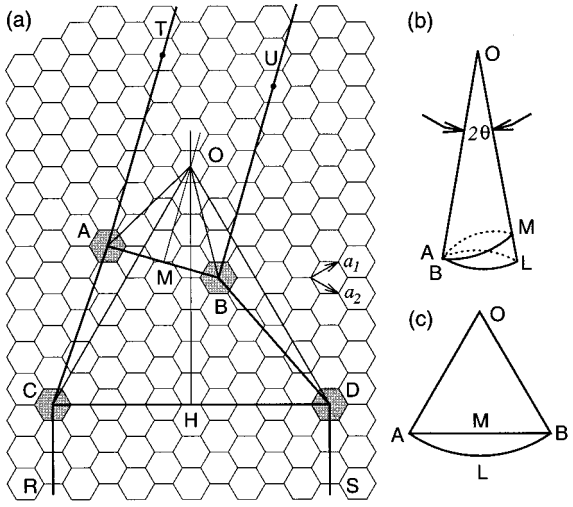

FIG. 1. (a) Projection map for the joint between two tubes. The chiral vectors for two tubes are shown by $\overrightarrow{AB}$ and $\overrightarrow{CD}$. The three-dimensional structure is obtained by connecting AT to BU, AC to BD, and CR to DS through cylindrical surfaces. A pentagon exists at the site C (or D) and a heptagon exists at A (or B). The joint region is uniquely expressed by a vector, $\overrightarrow{CA}$, which is given by Eq. (5). (b) The cone of $OALB$ and (c) its projection are shown in order to understand that the line AMB is a line of minimum length for going around the surface of the cone. $OM \perp AMB$ satisfies both (b) and (c).

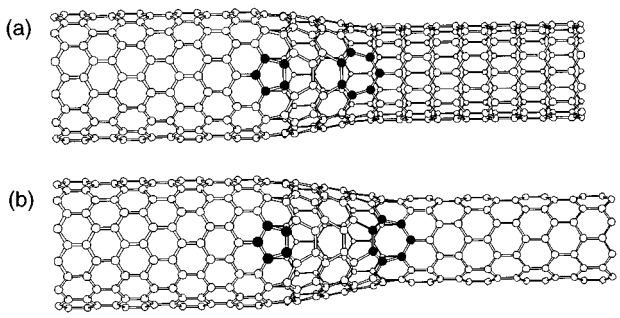

FIG. 2. (a) (12,0)-(9,0) and (b) (12,0)-(8,0) zigzag tubes are shown in which the carbon atoms of the pentagon and the heptagon are indicated by filled circles. Though we show only eight unit cells for each carbon nanotube, the calculation is performed for 16 unit cells. The total numbers of carbon atoms are (a) 735 and (b) 720, respectively.

many shapes for the junction between CN's in TEM experiments, in which the tube diameter increases or decreases as if two conical surfaces are shared with a common bottom surface.[10]

Recently coil-shaped nanotubes have been reported by several groups,[11–13] though the diameter of these multilayered tubes is large ($\sim$ 100 Å). The structure of the joint has been considered theoretically by introducing pentagons and heptagons at the inner and outer spiral tubule surfaces, respectively.[14] When the pitch of this spiral tube is zero, the tube will have a closed toroidal shape, which is considered to be stable theoretically.[14–18] However, no general discussions have been given for the structure for such a coil-shaped tube with a given distribution of pentagons and heptagons, as is clearly defined by a chiral vector in the case of a single-wall nanotube.[19] In the case of spiral nanotubes, a pentagon and heptagon pair is essential for understanding the joint between two carbon nanotubes.

Dunlap has discussed the joining of carbon nanotubes in the case that the pentagon and the heptagon in the pentagon-heptagon pair are on opposite sides of the tube.[20] In this case, the two-tubule axes bend by 30° with respect to each other in their projection map. Further, Dunlap introduced twists in the pentagon positions for the two nearest pentagon-heptagon pairs,[21] for understanding the coil-shaped tube.[21] We, however, found that the position of the pentagon and the heptagon in the pair discussed by Dunlap is a special case, though his geometry is one of the stable geometries. Here, we show the general case for a pentagon-heptagon pair and we further present a general rule, which is shown to satisfy the case discussed by Dunlap.

Very recently Akagi showed that the electronic structure of a spiral tube gives both metallic and semiconducting behavior,[22] though the general rule governing such behavior is still not well established. In this paper, we present a general formula for connecting two CN's and then we show calculated results of the tunneling conductance at the junction of two CN's.

In Sec. II, we present a three-dimensional structure for the joint between two carbon nanotubes by introducing a pentagon and heptagon pair, in which we introduce a wire-frame model for the axis of CN's defining the bond angles and the dihedral angle. Since we obtain a simple but geometrically strict rule for connecting two tubes, the definition is very useful not only for understanding the chirality of two joined tubes, as observed in TEM experiments, but also for designing possible, future mesoscopic devices. In Sec. III, we present calculated results of tunneling conductance for a metal-metal CN junction and a metal-semiconductor CN junction. We show the absence of conductance in the energy gap region for the metal-semiconductor CN junction.

II. PROJECTION METHOD FOR THE JOINT

It has been useful to use a projection mapping on the honeycomb lattice for describing the three-dimensional structure of the fullerene cage.[23] The projection from this map to the three-dimensional tubule surface is conformal in the sense that all bond angles for a hexagonal ring are fixed at $\pi/3$ (radians). Of course, there is distortion around the pentagon and heptagon causing changes in the bond length and bond angle. However, we assume that such distortions are very local around the pentagon and heptagon. Furthermore, the general idea presented here does not depend on the detailed bond angle and bond length, but only on the sp^2 connection of carbon atoms.

In Fig. 1, we show a projection map of two carbon nanotubes, which are given by rectangles $TABU$ and $RCDS$. The tubes, $TABU$ and $RCDS$, are uniquely determined by the chiral vectors, $\vec{AB}$ and $\vec{CD}$, respectively. The three-dimensional structure is obtained by connecting AT to BU, AC to BD, and CR to DS through cylindrical surfaces. When we roll up the projection map to make a tube, the chiral vectors correspond to the circumferential direction of the tubes and the translational vectors $\vec{AT}$ and $\vec{CR}$, which are perpendicular to $\vec{AB}$ and $\vec{CD}$, respectively, correspond to the directions of the tubule axes in three dimensions.

A polygon, $ACBD$, in the projection map denotes a joint, which connects two tubes, and the shape of the joint will be a part of a cone. Since the diameter of the tube $TABU$ is smaller than that of $RCDS$, we consider that a pentagon exists at the site C (or D) and a heptagon exists at A (or B). Since the solid angles of a pentagon and a heptagon in the fullerene are $2\pi-\pi/3$ and $2\pi+\pi/3$, respectively, the sum of the angles around the pentagon and the heptagon on the projection map should correspond to these angles. This fact gives $\angle ACR+\angle BDS=5\pi/3$ and $\angle CAT+\angle DBU=7\pi/3$. Further, when we use the fact, $\angle ACD+\angle BDC=2\pi/3$ and $AC=BD$, then $\vec{BD}$ is given by rotating $\vec{AC}$ around C by $\pi/3$. This condition gives the rule for connecting two tubes as discussed below.

First, we will give a formula for rotating a vector $\vec{v}_{n,m}=n\vec{a}_1+m\vec{a}_2\equiv(n,m)$ by $\pi/3$ on a honeycomb lattice. Denoting a $\pi/3$ rotation by $\mathcal{R}$, we get

$$\mathcal{R}\vec{a}_1=\vec{a}_1-\vec{a}_2,\mathcal{R}\vec{a}_2=\vec{a}_1. \tag{2}$$

Thus $\mathcal{R}\vec{v}_{n,m}$ is given by

$$\mathcal{R}\vec{v}_{n,m}=n(\vec{a}_1-\vec{a}_2)+m\vec{a}_1=\vec{v}_{n+m,-n}. \tag{3}$$

The formula of Eq. (3) for $\mathcal{R}\vec{v}_{n,m}$ will be used frequently in the following discussion.

Hereafter, we denote $\overrightarrow{CD}$, $\overrightarrow{AB}$, and $\overrightarrow{CA}$ as $\overrightarrow{CD}=\vec{C}_5=(n_5,m_5)$, $\overrightarrow{AB}=\vec{C}_7=(n_7,m_7)$, and $\overrightarrow{CA}=\vec{j}=(j_1,j_2)$, respectively, where n_5, m_5, n_7, m_7, j_1, and j_2 are integers. Then the condition for j_1 and j_2 for given $\vec{C}_5$ and $\vec{C}_7$ vectors is

$$\overrightarrow{DC}+\overrightarrow{CA}+\overrightarrow{AB}=-\vec{C}_5+\vec{j}+\vec{C}_7=\mathscr{R}\vec{j}=\overrightarrow{DB}. \tag{4}$$

Using Eq. (3), we obtain

$$(j_1,j_2)=(n_5+m_5-n_7-m_7,n_7-n_5). \tag{5}$$

Thus the joint vector, $\vec{j}$, is uniquely determined, once the two chiral vectors, $\vec{C}_5$ and $\vec{C}_7$ are given. Figure 1 is drawn for $\vec{C}_5=(5,5)$, and $\vec{C}_7=(1,3)$, which gives $\vec{j}=(6,-4)$, and $\mathscr{R}\vec{j}=(2,-6)$.

Next we consider the axis of the cone determined by $ACDB$. $ACDB$ is a part of a cone, the vertex of which is denoted by O in Fig. 1. In Figs. 1(b) and (c), we show a cone and its projection, respectively. For the cone, $OALB$, the line AMB is a line of minimum length for going around the surface of the cone, in which $OM\perp AMB$ satisfies both Figs. 1(b) and (c). We assume here that the lines AMB and CHD in Fig. 1(a) correspond to the minimum lines of the cone surface. This idea is valid, too, for the two tubes, $TABU$ and $RCDS$, where the lines AMB and CHD are minimum in length for going around the tubule surface. Thus this assumption seems to be reasonable. It should be mentioned here that the path AMB is an oval on the cone surface in three dimensions, while the path AMB is a circle on the tubule surface. Thus, we always expect some distortion arising from the oval shape from the cone section relative to the circle shape from the tubule surface. However, this fact does not affect the angle on the tube or cone surface, since the distortion is perpendicular to the surface.

Within this assumption, the vertex of the cone, O, is defined as the crossing of the two lines OM and OH, such that OM and OH are perpendicular bisectors of AB and CD, respectively. Since $OA=OB$, $OC=OD$, and $AC=BD$, the two triangles, $\triangle OAC\equiv\triangle OBD$, are identical to each other. Thus, $\angle ACO=\angle BDO$, which gives $\angle ACD+\angle BDC=\angle OCD+\angle ODC=2\pi/3$. Thus, we conclude that $\triangle OCD$ is a regular triangle. Similarly, since $\angle AOC=\angle BOD$, we have $\angle AOB=\angle COD=\pi/3$. Thus, $\triangle OAB$ is a regular triangle, too. The position of O is given by rotating $\overrightarrow{CD}$ or $\overrightarrow{AB}$ by $\pi/3$,

$$\overrightarrow{CO}=\mathscr{R}\overrightarrow{CD}=(n_5+m_5,-n_5),$$

$$\overrightarrow{AO}=\mathscr{R}\overrightarrow{AB}=(n_7+m_7,-n_7). \tag{6}$$

We can easily check from Eqs. (5) and (6) that $\overrightarrow{CO}-\overrightarrow{AO}=\vec{j}$.

When we define the angle of the vertex of the cone in three dimensions as 2θ, as is shown in Fig. 1(b), θ is given by

$$\theta=\sin^{-1}\frac{1}{6}\sim 9.594°. \tag{7}$$

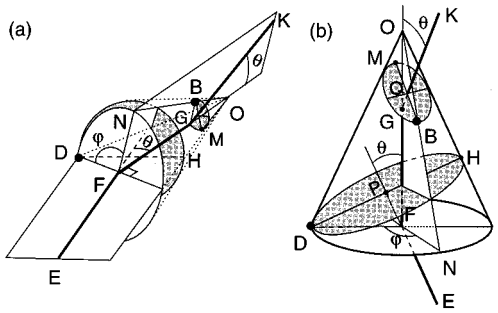

FIG. 3. (a) The dihedral angle, $\angle NFD=\varphi$ is defined between the two planes $\triangle OFD$ and $\triangle OFN$. Here, the axis of the cone, OF, is on both planes. FE and GK are the axes of the two nanotubes. It is noted that points O, F, D, and E are in a plane and that G, F, K, and N are in another single plane. The thick line $EFGK$ corresponds to a wire frame model for reproducing the axes for the tubes and the cone. D and B are the positions of the pentagon and the heptagon, respectively, in the joint region (see Fig. 1). The light shaded circle is the bottom surface of the cone and two dark shaded ovals are the cross sections between the cone and each tube. The crossing points of the cone axis with the tube axes, F and G are not located on these ovals. The bond angles, $\angle GFE$ and $\angle FGK$, are $\pi-\theta$. (b) Another view of the dihedral angle, φ, shown on the cone. Here, $DH\perp OH$ and $OM\perp MB$. P and Q are both centers of ovals.

The angle θ is the angle between the axis of the tube and that of the cone in three dimensions. If the points, O, B, and D in Fig. 1 lie on a line, the angle between the two axes of the tubes becomes zero, but when the pentagon and the heptagon are on opposite sides of the cone surface, then the angle between the two axes of the tubes becomes $2\theta=19.19°$.

When the pentagon and heptagon are neither along the same line nor on opposite sides of the cones, the two-tubule axes do not intersect with each other. In this case, we can define a dihedral angle, φ, between two planes as shown in Fig. 3. The two planes are defined by (1) the cone axis OF and an axis of the tube at the pentagon side FE, and (2) the cone axis OF and an axis of the tube at the heptagon side GK. The dihedral angle, φ, is defined by the rotation angle around the cone axis between $\triangle OFD$ and $\triangle OFN$, as shown in Figs. 3(a) and (b). The dihedral angle φ is relevant to the angle $\angle BOD=\Phi$ shown in the projection map of Fig. 1 as follows:

$$\varphi=2\pi\times\frac{\Phi}{\pi/3}=6\Phi, \tag{8}$$

where Φ is given by

$$\cos\Phi=\frac{|\vec{C}_5|^2+|\vec{C}_7|^2-|\vec{j}|^2}{2|\vec{C}_5|\cdot|\vec{C}_7|}. \tag{9}$$

Using Eq. (5), we can write the angles, Φ and φ, as a function of n_5, m_5, n_7, and m_7.

A general coiled-shape tube can be considered to connect many joints each with a pentagon-heptagon pair. The dihedral angle is a useful definition for understanding the three-dimensional structure of the two-tube axes and the single cone axis joining the carbon nanotubes. The definition of the

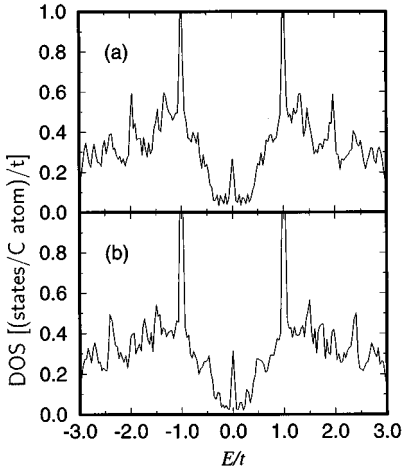

FIG. 4. Density of states of junctions for (a) (12,0)-(9,0) and (b) (12,0)-(8,0) zigzag tubes plotted in units per single carbon atom per energy t. All $E=0$ states correspond to edge states, the wave functions of which are localized not in the junction region, but at either end of the tubes.

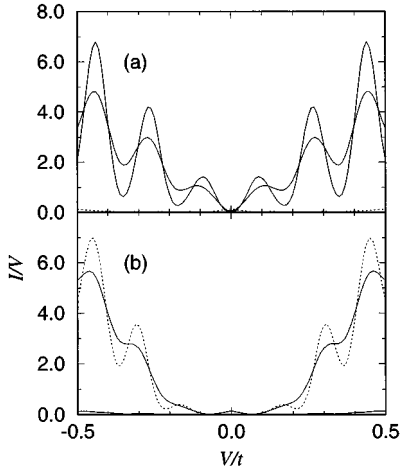

FIG. 5. Calculated conductance I/V for (a) (12,0)-(9,0) and (b) (12,0)-(8,0) zigzag CN, as a function of voltage V in units of t, using two different Gaussian broadening values, $\Delta E/t=0.33$ (solid line) and $\Delta E/t=0.50$ (dotted line). The estimated energy gap for the (8,0) semiconductor tube is $0.55t$.

dihedral angle is a good analogy to the chemistry, since the dihedral angle of a three-dimensional molecule is defined by three chemical bonds. The thick line $EFGK$ is a wire-frame model for representing the axes for the tubes and the cone.

When the dihedral angle φ is π, the positions of the pentagon and the heptagon (D and B in Fig. 3, respectively) are opposite to each other. In this case, the bending angle of the tubule axes in the projection map, which corresponds to Φ in Eq. (8), becomes $\pi/6$ (30°), which corresponds to the case discussed by Dunlap.[20,21] Here, we derive the condition for (n_5,m_5) and (n_7,m_7) in this special case and show that the condition satisfies the results of Dunlap (hereafter, denoted as $D94$).[20] In Fig. 1, OH is opposite the position of the pentagon (C or D), when we roll the projection map by connecting C to D, and R to S. Thus, the heptagon position A (or B) should be on the line OH. Using $\overrightarrow{OA}\perp\overrightarrow{CD}$ and Eq. (6), we can obtain the following equation:

$$n_5n_7+2n_5m_7-m_5n_7+m_5m_7=0 \quad (\text{when } \varphi=\pi). \tag{10}$$

When we set $n_7=12$ and $m_7=0$, we get $n_5=m_5$. This result corresponds to the results of Fig. 4 of $D94$. When we set $n_7=12$ and $m_7=-3$, we get $n_5:m_5=5:2$, which corresponds to the results of Fig. 5 of $D94$. It is noted here that (9,3) in the Fig. 5 of $D94$ corresponds to $(12,-3)$ using our definition. This comes about because of a difference in the definition of (n,m) for negative integers between our work and $D94$. For non-negative integers of (n,m), the definitions are the same. Thus, we show that the result of $D94$ is a special case of the present general case.

The points P and Q are both centers of the dark shaded ovals in Fig. 3(b) and P and Q are on the tube axes. The ovals are defined by rolling up AMB and CHD in Fig. 1 and thus $DH\perp OH$ and $OM\perp MB$ in Figs. 1 and 3. It is clearly seen from Fig. 3(b) that the P and Q are not crossing points of the tube axes with the cone axis, F and G. Thus, the tubule axis length on the pentagon side becomes shorter by PF in the wire frame model and the tubule axis length on the heptagon side becomes longer by GQ, where PF and GQ are given by

$$PF=|\vec{C}_5|\sin^2\theta, \quad GQ=|\vec{C}_7|\sin^2\theta. \tag{11}$$

The length of the cone axis FG is given by

$$FG=OF-OG=(|\vec{C}_5|-|\vec{C}_7|)\cos\theta. \tag{12}$$

Here, we use the fact that $OG\perp GB$.

Finally, we discuss the shape of the dark shaded ovals shown in Fig. 3(b). The bond angles, $\angle GFE$ and $\angle FGK$, are $\pi-\theta$, and these ovals have the same shape, but in different sizes. When we denote the longer and the shorter axis of the ovals as a and b, the ratio of b to a is given as a function of θ. After some calculation, b/a is given by

$$\frac{b}{a}=\left(1+\frac{4}{3}\sin^2\theta-\frac{2\sqrt{3}}{3}\tan\theta\right)^{1/2}\sim 0.918, \tag{13}$$

where we use Eq. (7). Thus, there is an 8.2% distortion at the cross section between the tubes and the cone. Using all formulas given here, the skeleton of the wire frame in three dimensions is well defined by only the four integers of two chiral vectors, n_5, m_5, n_7, and m_7. It is important to point out that there is no ambiguity in the structure of the junction if we specify the two chiral vectors of the tubes. Thus, the geometrically optimized structure or electronic structure of the connected tubes is uniquely described by the chiral vectors of the two nanotubes. In the next section, we consider some particular cases and their electronic structure.

III. TUNNELING CONDUCTANCE OF A JUNCTION

Here, we consider the tunneling conductance of a junction connecting two carbon nanotubes. As is discussed in the previous section, the structure of the junction is uniquely defined by two chiral vectors (n_5,m_5) and (n_7,m_7). Here, we

consider a large size cluster, which has a (n_5,m_5) tube, a (n_7,m_7) tube, and the junction region. Since we consider carbon nanotubes of finite length, all electronic states are given by discrete electronic levels. Here, we consider some Gaussian broadening for calculating the density of states and for calculating the conductance.

The structure of the junctions that we calculate here are the junctions between two zigzag tubes.[4] A zigzag tube defined by $(n,0)$ (n, integers) has one of the smallest unit cells among CN's and their electronic structure is either metallic or semiconducting depending on whether or not n is a multiple of 3, respectively. An armchair tube, (n,n), has an even smaller unit cell, but all armchair tubes are known to be metallic. Thus, zigzag tubes are suitable for considering a metal-semiconductor junction. In Fig. 2 we show a top view of (a) (12,0)-(9,0) and (b) (12,0)-(8,0) zigzag tubes, which are taken in the present paper as examples a metal-metal junction and a metal-semiconductor junction, respectively. Carbon atoms for the pentagon and the heptagon are indicated by filled circles. The corresponding junction vectors, (j_1,j_2), are given by $(3,-3)$ and $(4,-4)$, respectively. The dihedral angle φ is always zero in the case of a zigzag-zigzag CN junction. The three-dimensional lattice structure is given by formulas given in the previous section. The length of each carbon nanotube at both ends is taken as 16 unit cells in the calculation, while we show only eight unit cells in Fig. 2 for simplicity. Here, the unit vector of a zigzag tube is $\vec{a_2}$ if $\vec{a_1}$ is selected in the circumferential direction and the unit cells of each carbon nanotube start from the carbon atoms of the pentagon or the heptagon connected to each tube. The total numbers of carbon atoms are 735 and 720 for the (12,0)-(9,0) and (12,0)-(8,0) zigzag tubes, respectively.

The electronic structure is calculated by a simple tight-binding method in which only the nearest neighbor transfer energy, t, for π orbitals is considered. All the calculated energies are in units of t, whose value is known to be between 2.5 eV and 3.13 eV.[4] In the tight-binding calculation, we neglect for simplicity the other terms in the tight-binding expression and the hybridization, due to the curvature of the tube or junction. As explained in Sec. I, the effect of the curvature on the energy gap at the Fermi level is sufficiently small even for the smallest tubule diameter.[4] At the ends of the CN, we have dangling covalent π bonds, which give rise to edge states. Calculations show that the eigenfunctions of these edge states are localized only in the region about $6a$ ($a=|\vec{a}_1|$) from the tube end and their eigenvalues are always $E=0$. Since we use only the amplitude of the wave function in the junction, the effect of these edge states is automatically excluded in the conductance calculation.

The calculated results show that the eigenfunctions of the energy levels consist of contributions from (1) the delocalized wave function for the whole system, (2) the delocalized wave functions for each of the CN's and (3) edge states localized at the both ends. Since translational symmetry is broken at the junction, the Bloch wave functions of each CN are scattered by the pentagon, the heptagon, and the junction region of the tubes. If the energies of the wave functions in the two CN's are equal to each other, a delocalized wave function for the whole system is formed. Otherwise, a delocalized wave function in each tube region is formed. This situation is easily explained by the fact that the plane wave of an electron in reflected or transmitted at a positive square potential, which gives rise to a tunneling probability as a function of the electron energy. It is important to note that there are no localized states in the junction region, because the junction does not correspond to an attractive potential.

In Fig. 4, the density of states for (a) (12,0)-(9,0) and (b) (12,0)-(8,0) zigzag tubes is plotted in units per single carbon atom per energy t, as a function of energy in units of t. The energies of all eigenstates are within $|E/t|\leqslant 3$, which is consistent with three carbon bonds associated with each carbon atom. It is important to note again that all $E=0$ states (see Fig. 4) correspond to edge states, the wave functions of which are localized not in the junction region, but at both ends of the tubes. Thus, these states do not contribute to the conductance, though their energy is at the Fermi energy $E=0$. The density of states of these two-tube systems can be understood as the sum of the density of states of two CN's. We can see in the density of states (Fig. 4), not only the two-dimensional van Hove singularities of graphite at $E/t=\pm 1$, but also many one-dimensional $1/\sqrt{E}$ singularities, due to the one-dimensional energy bands, which are quantized in the circumferential direction.[4] Even when we remove the contribution of the localized states to the density of states, the resulting density of states is finite near the Fermi energy $E/t=0$, which indicates that one-dimensional metallic energy bands exist for both the (12,0) and (9,0) tubes.

In the case of the metal-semiconductor (12,0)-(8,0) zigzag nanotubes, the density of states near the Fermi energy is smaller than that of the (12,0)-(9,0) system, because of the absence of a finite density of states for the (8,0) CN near the Fermi energy. By calculating the energy levels of a (8,0) tube with the same length, we get an energy gap of $E_g/t=0.62$. Since we introduce Gaussian broadening, $\Delta E/t=0.033$, we see that the energy gap is reduced to $E_g/t=0.55$. In this case, the wave functions are only delocalized in the (12,0) tube region near the Fermi energy, and not in the (8,0) tube.

Using the eigenfunctions, we can calculate the conductance by calculating the current density. When a voltage V is applied to this system, the tunneling electric current, I, is given by[24]

$$I=2\pi e\hbar\int dE\{f(E)-f(E+eV)\}\times\sum_{ii'jj'}G_{i'i}(E)J_{ij}G_{jj'}(E+eV)J_{i'j'}. \tag{14}$$

Here, G is the imaginary part of the resolvent given by

$$G_{i'i}(E)=\sum_{\mu}C^{*}_{i'\mu}C_{i\mu}\delta(E-E_{\mu}), \tag{15}$$

where E_μ and $C_{i\mu}$ are the μth eigenvalue and ith component of the μth eigenfunction, respectively, which is obtained by solving the tight-binding Hamiltonian. J_{ij} is the current operator for atomic orbitals at i and j sites given by

$$J_{ij}=\frac{\hbar}{2m}\int_{S_0}dS\{\varphi_i\nabla\varphi^{*}_j-\varphi^{*}_i\nabla\varphi_i\}, \tag{16}$$

where φ_i is the ith atomic orbital, and the integration is taken at the same surface as for calculating the current density. Changing from a surface integral to a volume integral,[24] the J_{ij} is nonvanishing only for i and j at nearest neighbor sites, and in the region where the voltage changes between i and j sites. Here, we assume that it is only in the junction region that we expect a voltage drop. Since this tube junction system is so small, we consider the carbon network to be in the mesoscopic regime, in which electrons are not scattered in the periodic region, but only in the junction region. The tunneling current appears when the energy of the wave function to the left of the junction coincides with the energy plus eV of that to the right. This formulation may be valid even for delocalized wave functions over the whole region. When the voltage matches the tunneling condition for connecting delocalized wave functions over the whole region, the wave function that is then obtained should be approximated by a delocalized wave function at $V=0$.

In Fig. 5, we show the calculated conductance I/V for (a) (12,0)-(9,0) and (b) (12,0)-(8,0) zigzag CN's, as a function of applied voltage $-0.5<V/t<0.5$. Here, we use the two different Gaussian broadening values, $\Delta E/t=0.33$ (solid line) and $\Delta E/t=0.50$ (dotted line) for calculating $G_{ii'}$, etc. In the case of (a) metallic-metallic tubes, the conductance increases with increasing applied voltage. The oscillations in the conductance show the resonances in the tunneling probability between the two tubes, and these oscillations are closely related to the universal conductance fluctuations[25] recently reported in carbon nanotubes.[26] The increase of the conductance comes from the fact that (1) the resonance tunneling probability is proportional to V, if the density of states is constant near the Fermi energy and that (2) the current operator, J_{ij} is proportional to V. Again it is noted that there is no contribution from the edge states, which can be automatically excluded, because there is no amplitude of the wave function in the junction region.

In the case of (b) metal-semiconductor tubes, on the other hand, there is no conductance in the energy gap region for the semiconducting (8,0) tube though there is a finite density of states near the Fermi level. The results clearly show that a delocalized wave function is present near the Fermi level only in the metallic (12,0) tube region. Thus it is concluded that a semiconductor-metal junction is well established even in a nanoscale, mesoscopic structure.

When the length of the nanotube increases, there are more levels near the Fermi level. Thus, the amplitude of the oscillations will decrease relative to the absolute value of the tunneling conductance and the average level spacings will decrease in forming energy bands. The calculated results with larger energy broadening ΔE (dotted line in Fig. 5) are closer to this case compared to the case of smaller ΔE. However, if there is a defect in the tube, weak localization will make it possible to have a finite level spacing near the junction region, which gives rise to conductance fluctuations. This might be a possible reason for the observation of universal conductance fluctuations in carbon nanotube systems in which the region of the voltage drop corresponds to a disordered region.[25]

In conclusion, we present a general formula for connecting two CN's specified by the chiral vectors of the two tubes. The structure of the joint region is unique, given the chiral vectors of the two constituent CN's. The calculation of the conductance of metal-metal and metal-semiconductor tubes also shows resonant tunneling conductance effects. Especially for the metal-semiconductor CN system, we show the absence of conductance in the energy gap region of the semiconductor tube. This is evidence that two connected CN's can function as a nanometer size semiconductor junction device.

ACKNOWLEDGMENTS

The research at MIT was funded by NSF Grant No. DMR-95-10093. One of the authors (R.S.) acknowledges the Japan Society for the Promotion of Science for supporting his visit to MIT by the U.S.-Japan cooperative research program, and the MIT authors (G.D. and M.S.D.) acknowledge corresponding support by NSF INT 94-90144 from the U.S.-Japan program. Part of the work by R.S. was supported by a Grant-in Aid for Scientific Research in Priority Area ''Carbon Cluster'' (Area No. 234/05233214) from the Ministry of Education, Science and Culture, of Japan.

[1] S. Iijima, Nature (London) **354**, 56 (1991).
[2] M. S. Dresselhaus, G. Dresselhaus, and R. Saito, Phys. Rev. B **45**, 6234 (1992).
[3] J. W. Mintmire, B. I. Dunlap, and C. T. White, Phys. Rev. Lett. **68**, 631 (1992).
[4] Riichiro Saito, Mitsutaka Fujita, G. Dresselhaus, and M. S. Dresselhaus, Phys. Rev. B **46**, 1804 (1992).
[5] R. Saito, M. Fujita, G. Dresselhaus, and M. S. Dresselhaus, Appl. Phys. Lett. **60**, 2204 (1992).
[6] N. Hamada, S.-I. Sawada, and A. Oshiyama, Phys. Rev. Lett. **68**, 1579 (1992).
[7] K. Tanaka, M. Okada, K. Okahara, and T. Yamabe, Chem. Phys. Lett. **191**, 469 (1992).
[8] R. A. Jishi, D. Inomata, K. Nakao, M. S. Dresselhaus, and G. Dresselhaus, J. Phys. Soc. Jpn. **63**, 2252 (1994).
[9] S. Iijima, T. Ichihashi, and Y. Ando, Nature (London) **356**, 776 (1992).
[10] M. Endo, K. Takeuchi, K. Kobori, K. Takahashi, H. Kroto, and A. Sarkar, Carbon **33**, 873 (1995).
[11] X. B. Zhang, X. F. Zhang, D. Bernaerts, G. Van Tendeloo, S. Amelinckx, J. Van Landuyt, V. Ivanov, J. B. Nagy, Ph. Lambin, and A. A. Lucas, Europhys. Lett. **27**, 141 (1994).
[12] V. Ivanov, J. B. Nagy, Ph. Lambin, A. A. Lucas, X. B. Zhang, X. F. Zhang, D. Bernaerts, G. Van Tendeloo, S. Amelinckx, and J. Van Lunduyt, Chem. Phys. Lett. **223**, 329 (1994).
[13] C. H. Kiang, W. A. Goddard III, R. Beyers, J. R. Salem, and D. S. Bethune, J. Phys. Chem. **98**, 6612 (1994).
[14] B. I. Dunlap, Phys. Rev. B **46**, 1938 (1992).
[15] S. Itoh, S. Ihara, and J. Kitakami, Phys. Rev. B **47**, 1703 (1993).
[16] S. Ihara, S. Itoh, and J. Kitakami, Phys. Rev. B **48**, 5643 (1993).

[17] S. Ihara, S. Itoh, and J. Kitakami, Phys. Rev. B **47**, 12 908 (1993).
[18] J. K. Johnson, B. N. Davidson, M. R. Pederson, and J. Q. Broughton, Phys. Rev. B **50**, 17 575 (1994).
[19] M. S. Dresselhaus, G. Dresselhaus, and R. Saito, Carbon **33**, 883 (1995).
[20] B. I. Dunlap, Phys. Rev. B **49**, 5643 (1994).
[21] B. I. Dunlap, Phys. Rev. B **50**, 8143 (1994).
[22] K. Akagi, R. Tamura, M. Tsukada, S. Itoh, and S. Ihara, Phys. Rev. Lett. **74**, 2307 (1995).
[23] M. Fujita, R. Saito, G. Dresselhaus, and M. S. Dresselhaus, Phys. Rev. B **45**, 13 834 (1992).
[24] M. Tsukada and N. Shima, J. Phys. Soc. Jpn. **56**, 2875 (1987).
[25] P. A. Lee, A. D. Stone, and H. Fukuyama, Phys. Rev. B **35**, 1039 (1987).
[26] L. Langer, V. Bayot, J. P. Issi, L. Stockman, C. Van Haesendonck, Y. Bruynseraede, J. P. Heremans, and C. H. Olk, Phys. Rev. Lett. (to be published).